# Major findings in the third year of the project

In this report major findings in the third year of the project are presented, covering the period May 1, 2010 to April 30, 2011.

The prior reports on major findings are included at the end of this document

## 1. Evaluating the properties of data assimilation problem using MCMC inversion with 1D cloud resolving model and radar reflectivity observations

As mentioned in the section on major activities we have implemented a one-dimensional (1D) lagrangian cloud resolving model with MCMC (Markov Chain Monte Carlo) data assimilation algorithm (Posselt and Vukicevic, 2010) in order to evaluate properties of the radar reflectivity data assimilation problem with respect to the parameterized microphysical processes in terms of favorable conditions that would render the data assimilation problem better constrained and the solutions more accurate when using the data assimilation techniques such as 4DVAR or EnKF, which must be applied when a full-blown 3D atmospheric model with the microphysical parameterization is used. A progression of the nonlinear data assimilation problem toward well constrained formulation under varying conditions in the model and observations could be investigated thoroughly only by analysis of the full posterior PDF (Probability Density Function) solutions as shown in Posselt and Vukicevic (2010). Motivated by this approach, in the second year the new activity was started involving the implementation of the 1D model and MCMC algorithm at UM by graduate student van Lier-Walqui and diagnostic analysis of the microphysical processes in the model and simulation of the reflectivity from this model solutions.

In the third year a large number of experiments were conducted with MCMC algorithm and 1D model in the study on characterizing the properties of microphysical parameterization and the related data assimilation problem. The study results are presented in the new manuscript submitted for publication in Monthly Weather Review ("*Quantifcation of Cloud Microphysical Parameterization Uncertainty using Radar Reflectivity*", Van Lier-Walqui, Vukicevic and Posselt, 2011). In the following, the methodology and major findings of the study are summarized. The brief summary of the methodology is included in this section of the report on major findings to aid in better understanding of the study conclusions which are summarized in section (1b).

### *1a) Brief description of methodology*

The 1D lagrangian cloud model and the MCMC algorithm are described in detail in Posselt and Vukicevic (2010) and Vna Lier-Walquie et al. (2011). Only brief summary is presented here. The model is designed to emulate the changes in environment experienced by an atmospheric column as it moves through a cloud system following the mean flow. The vertical profiles of temperature and moisture are fixed and the model is driven by specified time-varying vertical profiles of vertical motion and water vapor tendency. Advection is only allowed to operate on cloud liquid and ice condensate, and only in the vertical direction. By varying the

vertical profiles of temperature, moisture, vertical motion, and water vapor forcing, the model can be adapted to simulate the flow through a range of different cloud systems. Since organized deep convection produces the bulk of the warm season precipitation globally, (and over the Great Plains in USA) and has been shown to be highly sensitive to changes in cloud microphysical parameters, an idealized representation of squall line type convection is simulated by the model. The added benefit to examination of squall-line type convection is that it contains two discrete cloud morphologies; convective, in which precipitation is primarily generated by the collision-coalescence (warm rain) process, and stratiform, in which the melting of snow and graupel play a key role. The model is run with 60 vertical layers with constant 250 meter vertical grid spacing and a 5 second timestep, and the radiative transfer, surface flux, and microphysical parameterizations are all identical to those used in the the NASA Goddard Cumulus Ensemble Model (Tao and Simpson 1993, Tao et al. 2003, Lang et al. 2007). Time series of rain from the model solution over 60 min is shown in Figs. 10 (equivalent to Figure 2a in Posselt and Vukicevic). It can be seen that the model produces realistic time-evolution of a squall-line with the convective phase followed by the stratiform phase.

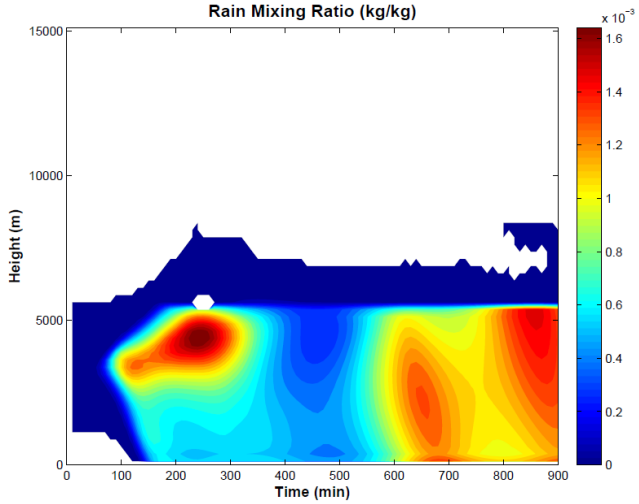


Figure 1: 1D Lagrangian model simulation of rain mixing ratio (kg/kg)

The project report in 2010 included the results from initial analysis of the model performance in the microphysical fields and illustration of the diagnostics that would be used in further analysis and data assimilation with the MCMC system. In the initial analysis we used Simulation of reflectivity and polarimetric differential reflectivity (SimPolRad) model to simulate reflectivity data to use in the data assimilation experiments. Although, the results using this radar-reflecivity model were satisfactory in terms of producing realistic reflecivity fields it was found, as noed in the last year project report, that the software was computationally inefficient for use in the data assimilation. We have investigated several options toward improving the efficiency of SimPolRad but none have shown sufficient reduction in computing time to render feasible application with MCMC data assimilation algorithm, which by design requires millions of model simulations. We replaced SimPolRad with Quickbeam radar for-ward operator (Haynes et al. 2007) for a 3 GHz radar frequency (comparable to WSR-88D radar frequency). This new operator produced very similar radar reflectivity simulations to SimPolRad but with significantly higher efficiency. Quickbeam is capable of solving Mie

equations for a variety of radar frequencies and a variety of user-specified particle size distributions and microphysical parameter values. In contrast to the work of Tong and Xue (2008), the perturbed values of the microphysical parameters are used in the radar forward operator. In this sense, the cloud microphysics model and the radar forward operator can be thought of as constituting a single, consistent forward model. In tests (not shown here), Quickbeam was found to be also comparable to other available forward operators such as SDSU (Masunaga et al. 2010) in relative distribution of reflectivity, with the exception of the melting layer reflectivity bright-band, which Quickbeam is unable to reproduce. Radar reflectivity is simulated at model grid resolution and beam bending, broadening and attenuation are not considered due to the idealized nature of the investigation. From this solution measurements are selected from two distinct storm morphological regimes: convective at 60 minutes and stratiform at 120 minutes.

In MCMC experiments ten microphysical parameters are chosen for their importance within the equations describing microphysical processes; these parameters are listed in Table 1. For each parameter, a minimum and maximum realistic value is defined as well as a `truth' value. When the model is integrated using this choice of parameters, the results are considered the synthetic true state of the atmosphere, and simulated observations of this model state are deemed observational truth (this is represented in gray in the schematic shown in Figure 2). As with real observations, the simulated observation is stochastic, and can be defined by a PDF. Assuming a Gaussian distribution for the observational uncertainty, this PDF is defined by two quantities { the mean, or _rst moment, and the covariance, or second moment. The observational truth is used to define the mean, implying unbiased observations. The observations were assigned a multi level error covariance which was simulated explicitly from a large Monte Carlo ensemble that was based on Posselt and Vukicevic (2010) simulations. The choice of the microphysical parameters of interest defines a ten-dimensional control parameter space. This space is explored so as to determine the ten-dimensional probability density function of the parameters conditioned on information in the observations.

TABLE 1. Cloud microphysical parameter descriptions, abbreviation, along with truth values and parameter ranges. Table reproduced from PV10.

| Parameter description | Abbreviation | Units | Truth | Min | Max |
|---|---|---|---|---|---|
| Snow fall speed coefficient | $a_s$ | $\text{cm}^{1-b_s}$ | 200.0 | 50.0 | 1000.0 |
| Snow fall speed exponent | $b_s$ | none | 0.3 | 0.1 | 1.0 |
| Graupel fall speed coefficient | $a_g$ | $\text{cm}^{1-b_g}$ | 400.0 | 50.0 | 1200.0 |
| Graupel fall speed exponent | $b_g$ | none | 0.4 | 0.1 | 0.9 |
| Intercept parameter of the rain particle size distribution | $N_{0r}$ | $\text{cm}^{-4}$ | 0.5 | 0.0 | 5.0 |
| Intercept parameter of the snow particle size distribution | $N_{0s}$ | $\text{cm}^{-4}$ | 0.5 | 0.0 | 5.0 |
| Intercept parameter of the graupel particle size distribution | $N_{0g}$ | $\text{cm}^{-4}$ | 0.5 | 0.0 | 5.0 |
| Snow particle density | $\rho_s$ | $\text{g cm}^{-3}$ | 0.2 | 0.1 | 1.0 |
| Graupel particle density | $\rho_g$ | $\text{g cm}^{-3}$ | 0.4 | 0.1 | 1.0 |
| Threshold cloud mass mixing ratio for autoconversion to rain | $q_{c0}$ | $\text{g kg}^{-1}$ | 1.0 | 0.1 | 3.0 |

Although only microphysical parameters were directly perturbed, all model variables and simulated observations affected by these perturbations are also described by a probability density function under the constraints of the model-observational system. In the results the ten-dimensional parameter PDFs are presented as well as joint PDFs of parameters and observations,

parameters and microphysical process activity, and microphysical process activity PDFs. The ten-dimensional posterior microphysical parameter PDF represent the solution to the inverse problem and provides robust estimates of uncertainty in the parameters when constrained by the radar reflectivity observations. In order to illuminate observational constraint in the data assimilation which results from the relationship between parameters and observations by the models, posterior PDFs of the joint parameter-observation space are then analyzed. These PDFs show the sensitivity of radar reflectivity simulated observations to simultaneous perturbation of microphysical parameters; in addition, they illustrate which vertical levels provide observational constraint to each parameter. Then, in order to determine why observations are sensitive to perturbations in microphysical parameters, joint PDFs of microphysical parameters and activity of individual microphysical processes within the parameterization scheme are evaluated. The microphysical processes included in this analyses are listed in Table 2. The process-activity PDFs demonstrate the actual microphysical response to simultaneous perturbation of the ten microphysical parameters and yield insight into how parameter perturbation affects modeled cloud microphysics. From these, the conclusions are finally derived about the approach to stochastic modeling of the processes by controlling the processes directly and not by the choice of physical parameters. These conclusions present basis for the next and final phase of the project.

TABLE 3. Microphysical process descriptions, abbreviation, source and product hydrometeors of the process. Note that ERN, the evaporation of rain, is a negative definite quantity and here only the absolute value is shown.

| Process description | Abbreviation | Source | Product |
|---|---|---|---|
| Evaporation of rain (negative) | ERN | Rain | Water Vapor |
| Melting of snow | PSMLT | Snow | Rain |
| Melting of graupel | PGMLT | Graupel | Rain |
| Cloud ice accretion of rain | PIACR | Cloud Ice, Rain | Snow, Graupel |
| Graupel accretion of rain | DGACR | Graupel, Rain | Graupel |
| Snow accretion of rain | PSACR | Rain, Snow | Snow, Graupel |
| Autoconversion of cloud water to rain | PRAUT | Cloud water | Rain |
| Rain accretion of cloud water | PRACW | Rain, Cloud water | Rain |
| Graupel accretion of cloud water to produce rain | QGACW | Graupel, Cloud water | Rain |
| Rain accretion of snow | QRACS | Rain, Snow | Rain |
| Deposition on snow | PGDEP | Water Vapor,Snow | Snow |
| Snow accretion of cloud water | PSACW | Cloud water, Snow | Snow, Graupel |
| Bergeron process (deposition/riming) | PSFW | Cloud water | Snow |
| Deposition on graupel | PGDEP | Water vapor | Graupel |
| Graupel accretion of cloud water | DGACW | Graupel, Cloud water | Graupel |

***1b) Major findings of the study on quantifcation of cloud microphysical parameterization uncertainty using radar reflectivity***

Radar reflectivity observations are shown to more tightly constrain microphysical parameter uncertainty than the column-integral observations used in Posselt and Vukicevic (2010) { reducing variance and in some cases eliminating biases in the parameter inversion. In

particular, ice fall speed parameters and intercept parameters of hydrometeor particle size distribution are shown to be considerably better constrained by radar reflectivity observations (Figure 2). Non-uniqueness shown by PV10 in the inverse solution for ice hydrometeor fall speed parameters is eliminated with the use of radar reflectivity, although the posterior PDF for cloud water-to-rain auto-conversion threshold shows a bimodal structure which was not observed in PV10 for column-integral observations { a sign of non-uniqueness in the inverse solution. This property is a likely consequence of microphysical processes which serve to compensate for modified hydrometeor concentration associated with the spurious mode of this parameter. These results demonstrate the increased information content of radar reflectivity relative to column-integral measurements as well as the utility of the probabilistic analyses employed.

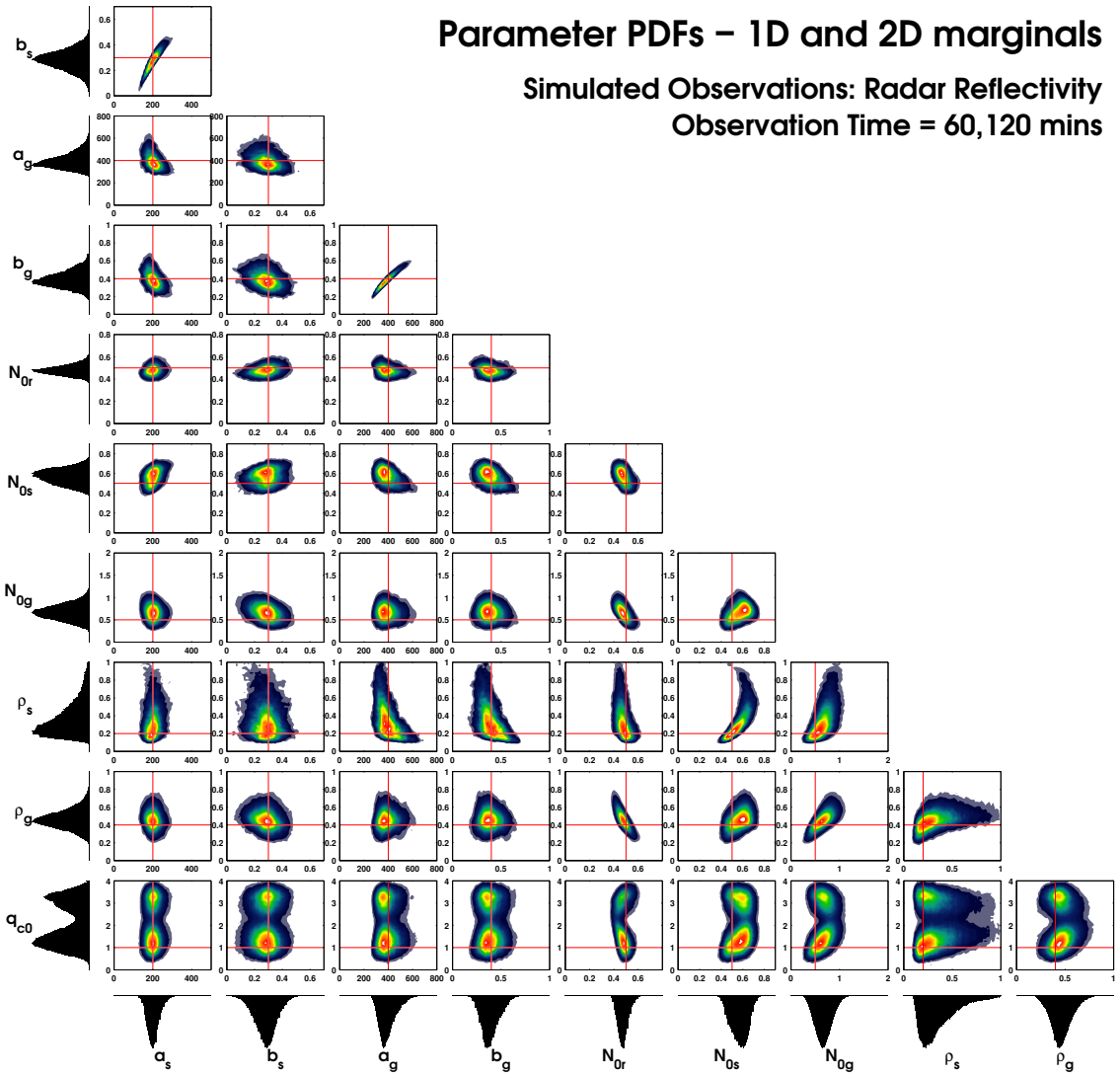


Figure 2: 1D Lagrangian model simulation of rain mixing ratio (kg/kg)

Interpretation of microphysical parameter uncertainty under the constraint of radar reflectivity is then facilitated by a number of novel analyses. Joint parameter-observation PDFs allow for a diagnosis of what observational levels constrain parameter uncertainty. It is found that in many cases, these relationships yield to intuitive analysis, while in other cases, sensitivity

of observation to parameter perturbation is likely the product of complex microphysical interactions (Figure 3). For example, evaporation of rain, graupel accretion of rain, and rain accretion of cloud water are shown to change the sign of their first order relationship with all parameters between the stratiform and convective storm regimes. These analyses also underscore the value of a vertically resolved observable quantity { in many cases the relationship between reflectivity and parameter perturbation is strongly height-dependent.

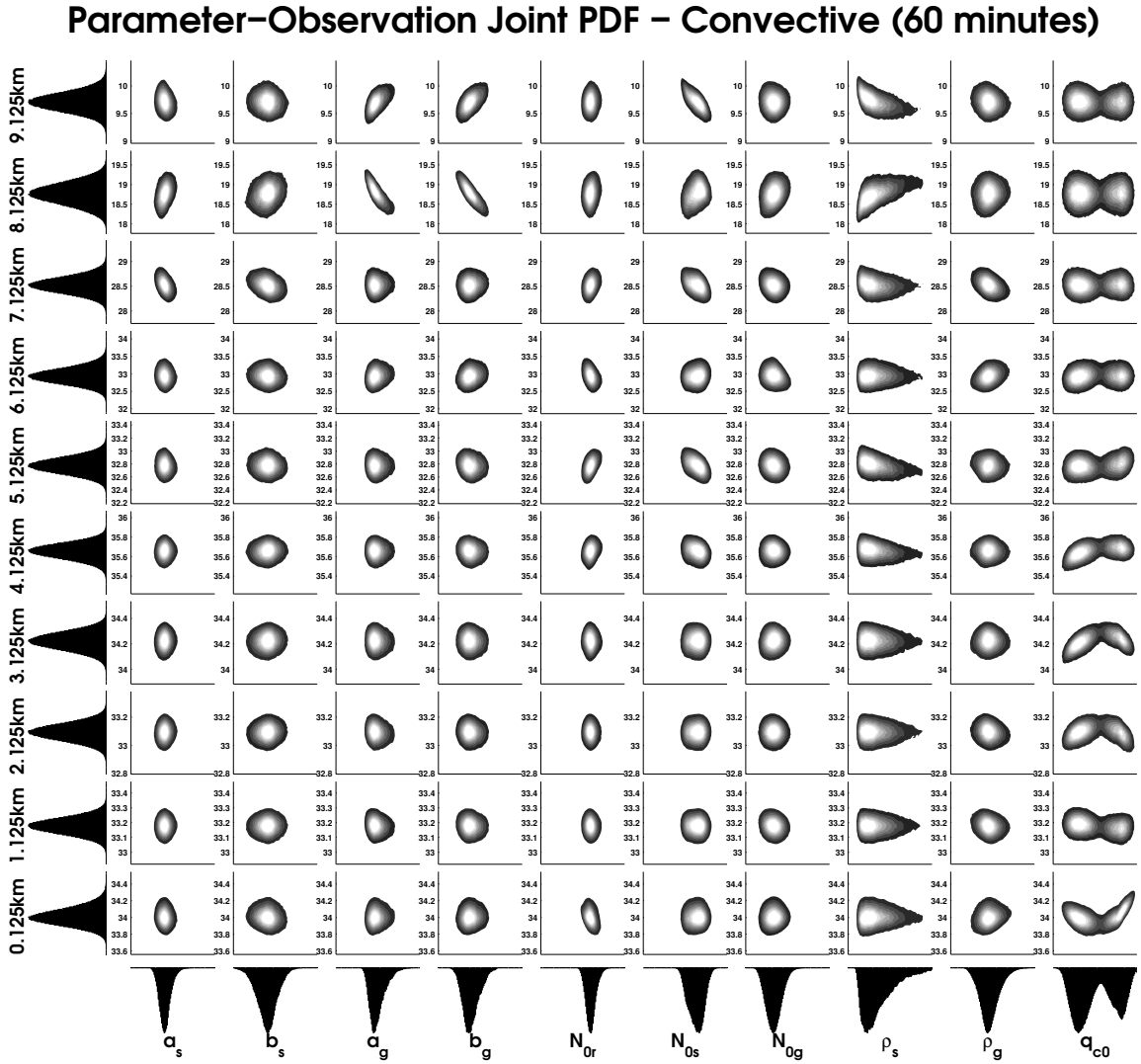


Figure 3A: Joint PDF of parameter and radar reflectivity observations at various vertical for a time *during convective* phase of simulated squall-line. Each row corresponds to simulated reflectivity at a particular model level, whereas each column corresponds to a different model physics parameter.

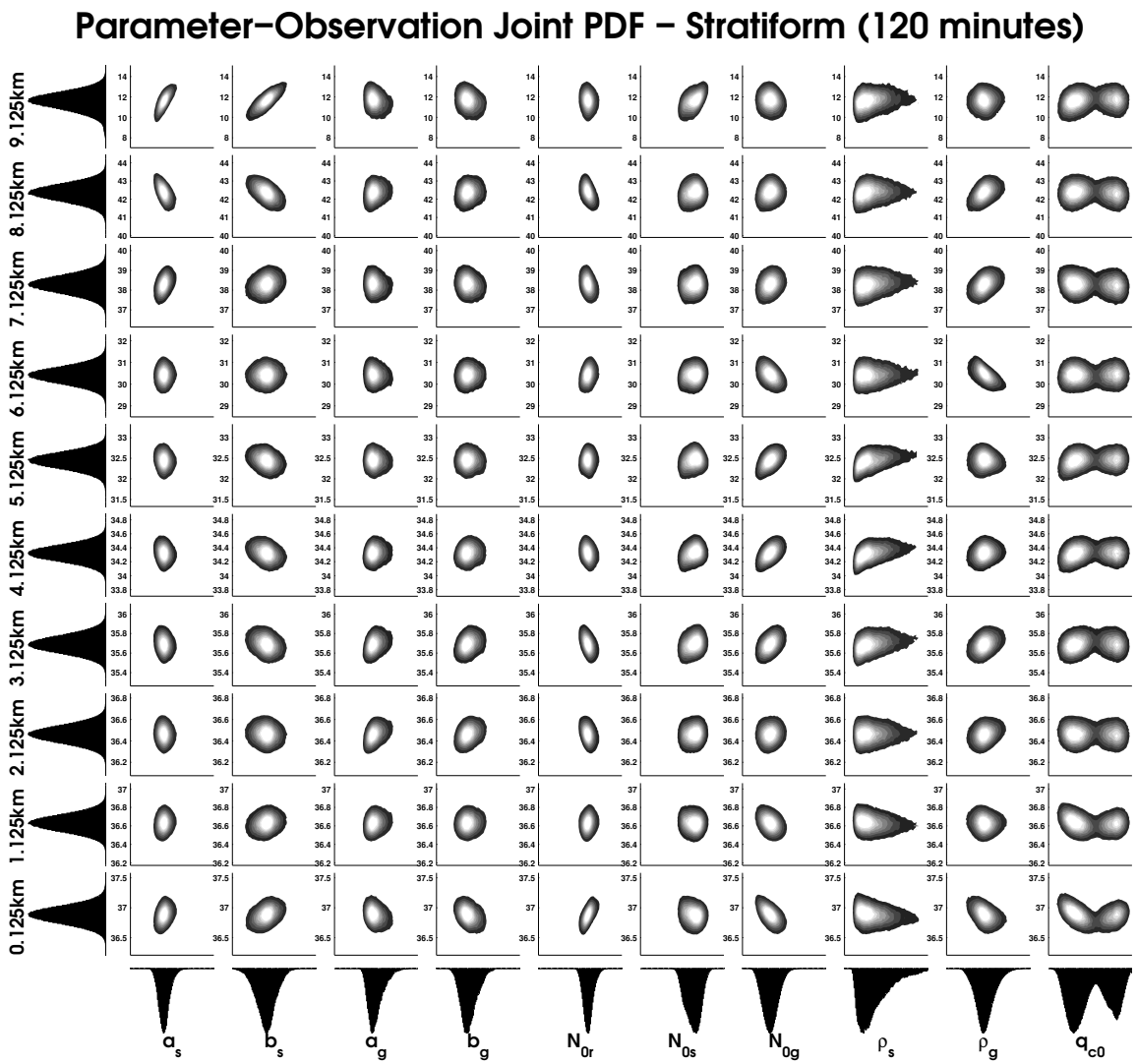


Figure 3B: Joint PDF of parameter and radar reflectivity observations at various vertical for a time *during stratiform* phase of simulated squall-line. Each row corresponds to simulated reflectivity at a particular model level, whereas each column corresponds to a different model physics parameter.

Finally, PDFs of microphysical process activity are produced in order to further analyze the processes which contribute to the microphysical state, and thus, the observable state of the model. The activity of a number of microphysical processes are integrated over times in the convective and stratiform regimes and treated probabilistically. The results show that the behavior of microphysical processes and the relationship between uncertainty in parameters and microphysical processes is strongly dependent on storm morphology. For example, the relationship between graupel accretion of cloud water and rain accretion of cloud water changes its sign between convective and stratiform storm regimes. This is an indication that in different storm morphological regimes, distinct microphysical processes and hydrometeor types may provide the primary constraint on microphysical behavior (Figure 4).

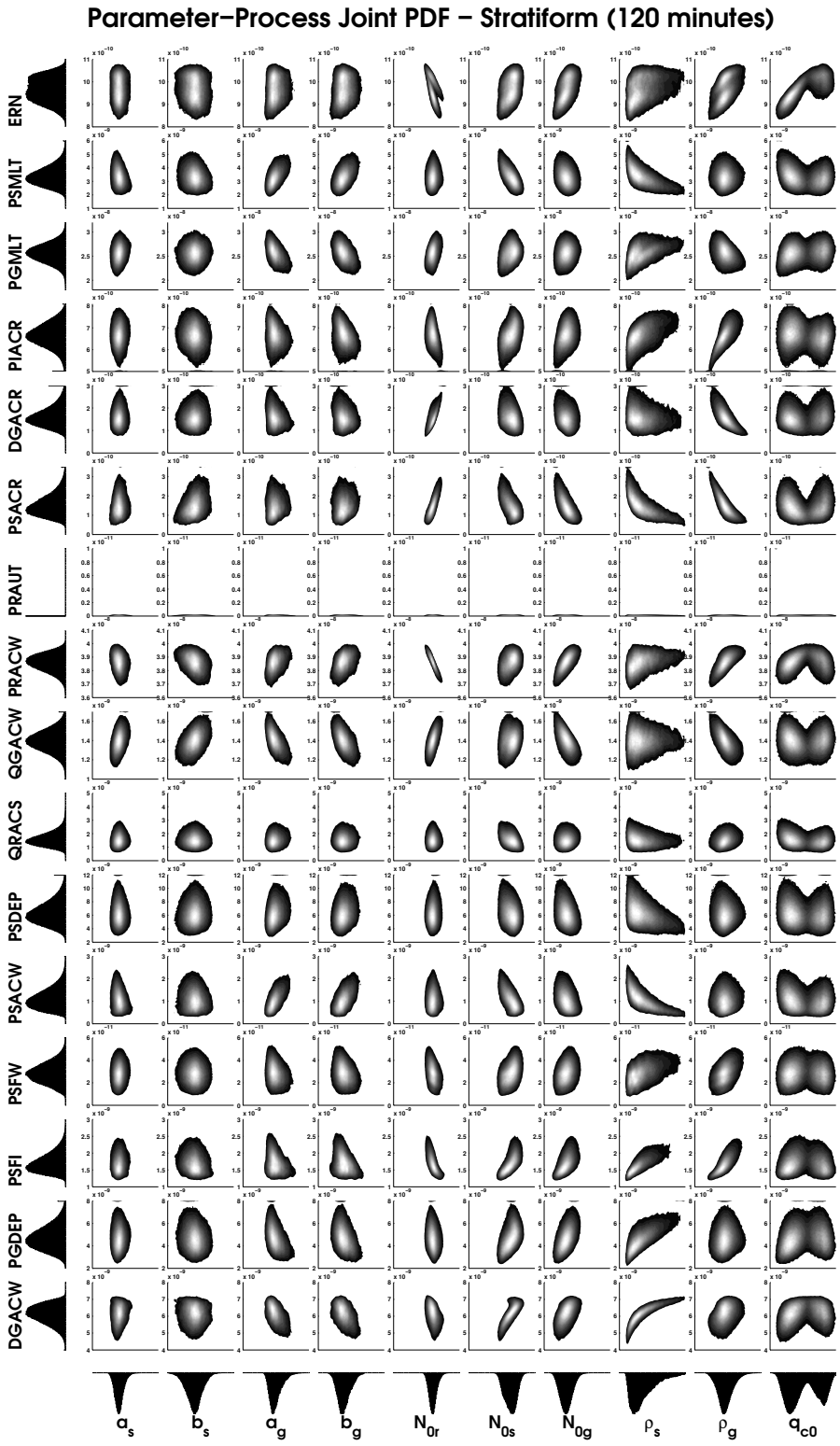


Figure 4 A: Joint PDF of parameters and microphysical process activity during convective phase of squall-line development. Each row represents a spatio-temporal integral of process activity while each column represents a microphysical parameter.

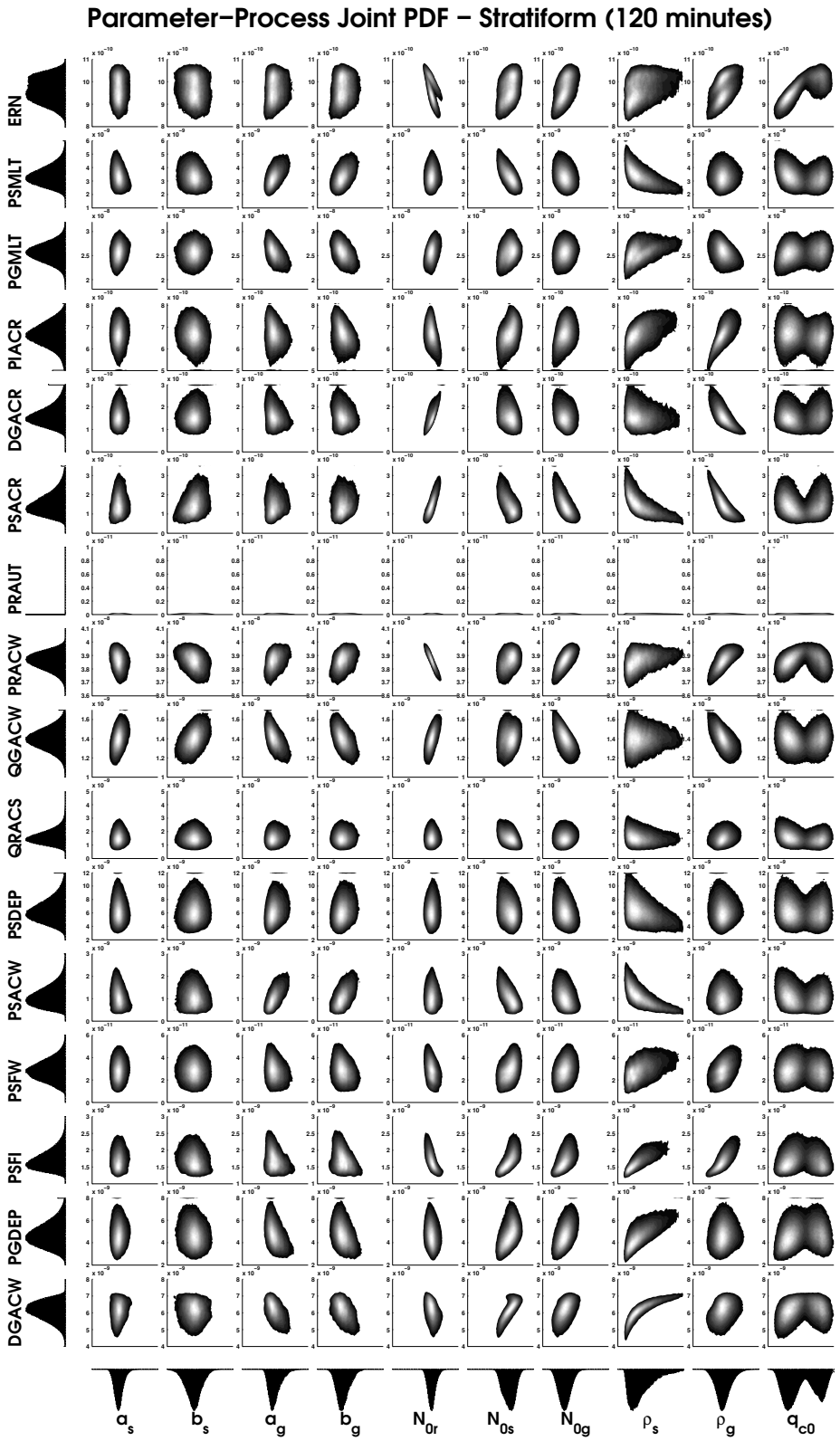


Figure 4 B: As in 4A, for process activity during stratiform phase of squall-line development.

The PDF, fully in process space, allows for observation of the interrelationships between microphysical processes.(Figure 5). The shape of these distributions (the number of modes, skewness and linearity of interrelationships) provides insight into the ease with which microphysical uncertainty might be represented in a parameterization scheme. Specifically, the greater the degree to which the PDF resembles a multivariate Gaussian distribution, the easier this uncertainty might be stochastically reproduced. The current results show that microphysical process PDFs appear to be more “well behaved" than parameter PDFs,.This suggests that a stochastic representation of microphysical processes may more closely describe microphysical parameterization uncertainty than a stochastic representation of microphysical parameters. In the current study, however, microphysical process PDFs are limited by the fact that it is parameters, and not processes, which are directly perturbed.

In the next study (already ongoing at the time of writing this report) we will investigate inversions with individual as well as multiple microphysical processes as control parameters using MCMC experiments. The results would be then related to the more practical data assimilation approaches such as 4DVAR and EnKF by evaluating the maximum likelihood (equivalent to 4DVAR solution), and mean and covariance (equivalent to EnKF solution), which would be derived from the full PDF solutions. These results would provide specific guidance for applications of the method of stochastic adjustment of microphysical processes in 3D atmospheric models with the standard data assimilation techniques.

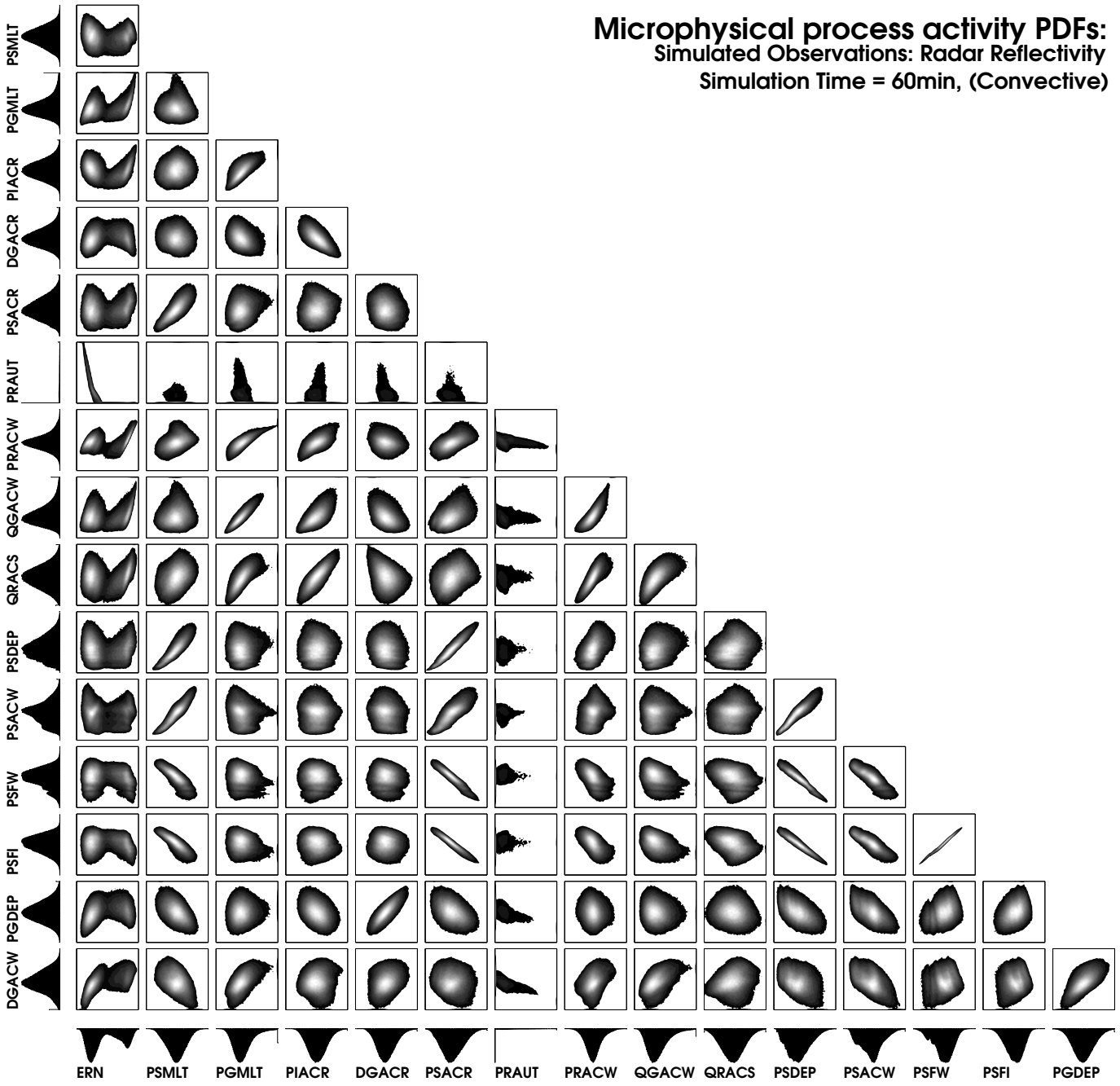


Figure 5A: Joint PDF of microphysical process activity during the convective phase of the squall-line development (40-80 minutes)

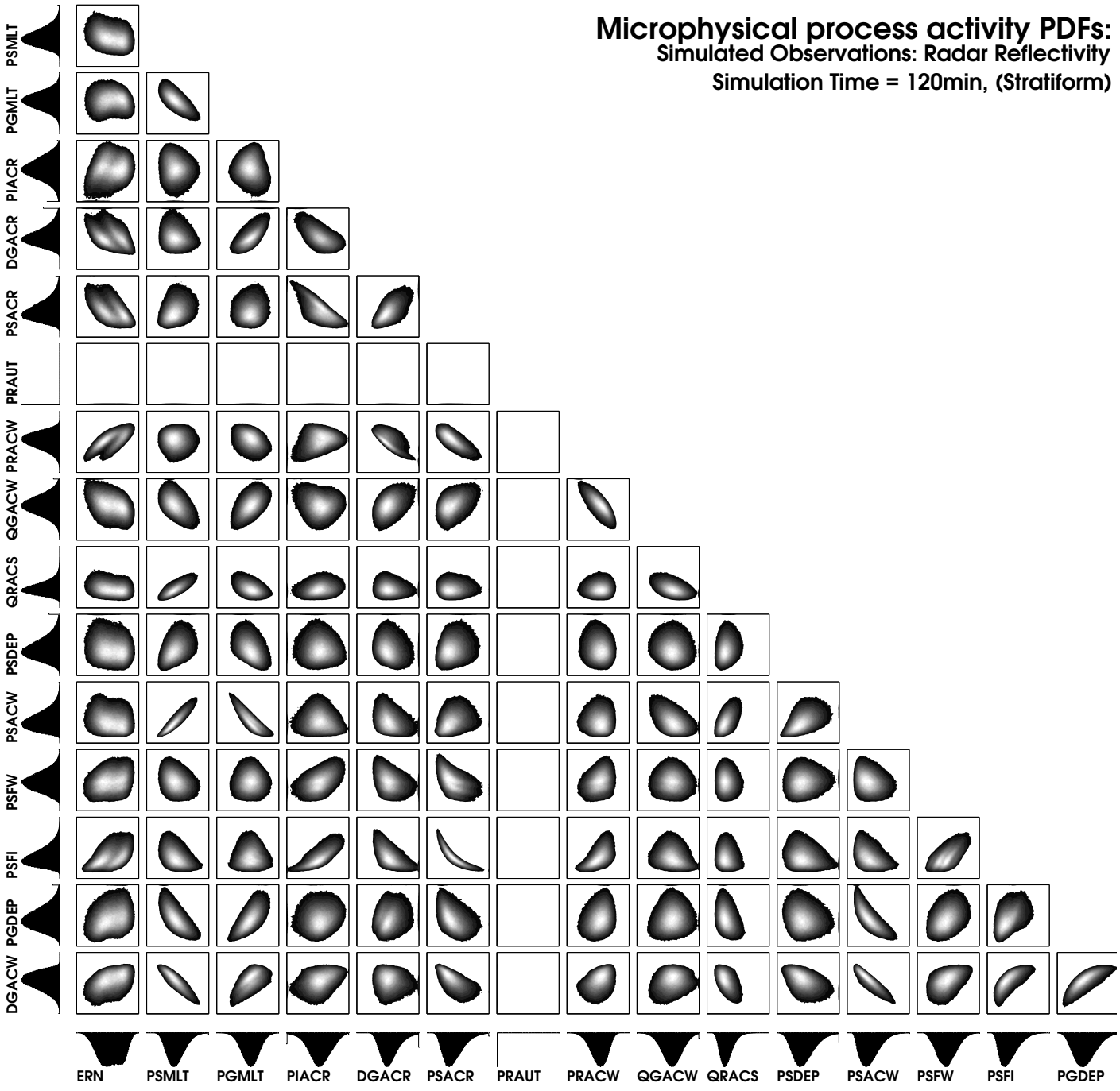


Figure 5B: As in 5A, for microphysical process activity during the stratiform phase of the squall-line development (100-140 minutes)

**Major findings in the second year of the project were in the following areas**

**1.** Mesoscale model simulations, verification and sensitivity to modeling of radar reflectivity

**2.** Evaluating the data assimilation approach using MCMC with 1D cloud resolving model

## 2. Mesoscale model simulations, verification and sensitivity to modeling of radar reflectivity

The verification of WRF-ARW high resolution forecasts were performed for two IHOP events. The selected events occurred on June the 13$^{th}$ and June the 16$^{th}$ of 2002. The June 13$^{th}$ event was associated with a stationary/cold frontal boundary and characterized by elevated convection. At the simulation initial time, 00 UTC, multiple convective cells existed in the vicinity of Oklahoma northern border. These convective cells quickly organized into a squall line that moved north-west to south-east over the state of Oklahoma. The June 16$^{th}$ 2002 event was also initialized at 00 UTC. At the initial time the event was characterized by well defined meso-scale convective system (MCS) in southern KS and northern OK. The MCS developed from the merger of three smaller systems couple of hours earlier.

Simulations of the two events were performed over six hour periods, using 2-km horizontal grid spacing and 53 vertical levels and three different microphysics schemes. The three microphysics included Lin, WSM6 and Schultz. The forecast was transformed into equivalent of 3D radar reflectivity fields using "Kessler" and "RAMS" reflectivity models (described briefly in the major activities). Simulations with the more sophisticated SynPolRad model were not completed by the time of this report due to computational difficulties. This model code is very inefficient as currently implemented and would need to be optimized before it could be effectively applied to large data sets such as those from the high resolution simulations by WRF-ARW model. The current results with the high resolution simulations in the radar reflectivity space include 6 model realizations at each verification time, corresponding to the three different microphysics schemes and the two reflectivity calculation options.

For each case the observation-based LAPS analysis was produced, using the same spatial and temporal resolutions as the numerical model simulations. For this purpose all available observations including both 2D and 3D radar data reflectivity, radial velocities, other in-situ and

remotely sensed data were used. The model runs used LAPS diabatic analysis as initial conditions. The forecast verification included only comparison between the model synthetic reflectivity and the equivalent from the LAPS analysis using different skill scores.

Firstly, the skill scores of the two different synthetic reflectivity calculations were compared. The results for different reflectivity thresholds are presented in Figures 1 and 2 on the example of two microphysical parameterizations and for the case of June 13. In the case of Lin microphysics RAMS calculation of reflectivity is characterized by larger bias (ratio between number of observed and forecasted points) for all three different thresholds (20, 30 and 40 dBZ). Also, bias values increased with an increase in the reflectivity threshold (Fig. 1). Despite difference in bias, the two different approaches resulted in almost identical equitable threat score (ETS) values (Fig. 2). The same analysis using the Schultz microphysics shows similar results in terms of sensitivity of the diagnostics to the reflectivity model (Figs.1 and 2).

Skill measures calculated by using only the Kessler approach for three different microphysics and for the same thresholds are shown in Figures 3 and 4. It can be seen that changing the microphysics resulted in a notable difference in bias (fig. 3). The Lin scheme was frequently characterized with the highest bias, while opposite was true for the Schultz microphysics. All model simulations had comparable skill for all thresholds (Fig. 4). As expected the skill in all model solutions decreased with lead time. Overall, for June the 13$^{th}$ 2002 event Lin microphysics solution resulted in bias larger than other solutions for almost all times and for all thresholds. This was especially true when compared to model solution using the Schultz microphysics.

Figure 5 shows a west-east cross section of simulated reflectivity for the two schemes and the two different reflectivity calculation approaches. The overlaid contours represent the hydrometeor type and content. The fact that RAMS radar reflectivity calculation approach resulted in notably larger bias compared to the Kessler approach for Lin microphysics (Figs. 5a and b) pointed toward a Lin microphysics's characteristic, large graupel production (Jankov et al. 2009). Namely, the RAMS approach weights each ice component (snow, cloud ice and graupel) separately and graupel being a larger particle size is weighted more heavily than others. Given the Lin microphysics' tendency to largely overestimate presence of graupel, the RAMS approach resulted in much larger bias compared with the Kessler approach (Figs. 5a and b). In contrast, for Schultz microphysics, which is characterized by very limited graupel production (Jankov et al.

2009), different approaches in reflectivity calculation did not impact the results much (Figs. 5c and d).

Similar analyses were performed for June the 16th 2002 event. Bias calculation for the Lin and the Schultz schemes for lower thresholds show much less sensitivity to the choice of synthetic reflectivity calculation (Fig. 6). For 40dBZ threshold RAMS option was characterized by higher bias at all times compared to the Kessler option. Also, higher threshold comparison pointed toward higher bias for Schultz scheme which was opposite from findings for the June the 13th 2002 event. However, the ETS values for the two approaches were comparable for all times and all thresholds (not shown). A similar trend in bias and ETS values was observed when various microphysical schemes were compared (Fig. 7). For this event the large differences in bias were not detected among schemes at lower thresholds. For a 40 dBZ threshold the WSM6 solution is characterized by highest bias at all times, followed by Schultz and Lin. ETS values were comparable for all solutions at all times and for all thresholds.

Lastly, the contour frequency height diagrams were evaluated for the model and LAPS analysis and compared. These diagrams form bases for computing the cost function that would be used in the assimilation of reflectivity and that would represent systematic errors in vertical distribution of hydrometeor mass by the microphysical processes. Figure 8 illustrated the reflectivity-height histograms for simulation using the Lin microphysics for two reflectivity calculation approaches (Figs 8a and b) and simulation using the Schultz microphysics with the Kessler calculation approach (Fig. 8c) for the first three forecast hours. Once again, it can be seen that the RAMS calculation approach puts more weight and higher reflectivity on ice particles, especially larger ones, such us graupel. Comparison of the two different microphysics (Lin and Schultz) using the same Kessler reflectivity calculation approach, points toward larger frequency of occurrence at higher levels for the Lin scheme simulation as opposed to the Schultz simulation. Also, for this event, the frequency of occurrence seem to be larger for the Lin simulation at all heights and for all ranges of reflectivity intensity. This indicates larger presence of graupel in the case of Lin microphysics but also potentially explaining very limited trailing stratiform region in the case of the simulation using Schultz microphysics (Figs. 8b and c).

Similarly, Figure 9 shows all three model solutions for the first and the third forecast hours for June the 16th 2002 event. It can be seen that for this event the Lin solution was characterized by lower frequency of occurrence at higher and mid levels and 20-40 dBZ

reflectivity range. This agrees well with previously discussed bias and ETS analysis. Also, WSM6 solution was very comparable to the one using Schultz microphysics.

In summary the analysis of the two convective events indicate, not surprisingly, that the numerical model at the resolution of 2 km does not handle well events characterized by non-organized convection (single convective cells). Also, in this case as the convection got organized different microphysics performed differently (e. g. Lin was more active than other microphysics, particularly in terms of ice production). On the other hand, for the event in which the convection was well organized at the model's initial time, various model solutions ended up with comparable results. Solution using the Schultz microphysics failed to simulate trailing stratiform region, while in the case of the Lin microphysics solution the stratiform region was overestimated. At the same time all model options resulted in a very similar solution for the well developed convective line. Animations of 6 and 3-hr simulated reflectivity and the corresponding analysis with 15 min. interval for June the 13$^{th}$ 2002 and June the 16$^{th}$ 2002 events, respectively can be found at the following location: http://laps.noaa.gov/nxgn/. The file names are 13frames700_20020616_lin_kess.gif and 21frames_20020613_lin_kess.gif. These results suggests that when the phase errors are small, the different microphysical schemes exhibit compatible systematic errors, but not exactly the same. Correcting of such errors should be feasible by the data approach that is under development in the current study.

The major funding from the current WRF-ARW model validation with respect to the assimilation of the radar reflectivity observations, is that the systematic errors in vertical distribution and intensity of reflectivity, which would be used to define the cost function for improving the microphysics results and the associated precipitation forecast, are equally or more sensitive to the reflectivity model used than to the choice of microphysics parameterization. This result implies that the errors in the observation operator could dominate the background errors in the assimilation and suggests that better than relatively simple empirically-based reflectivity model should be used. One such model is the SynPolRad that is still not properly tested in the current study due to the computational inefficiency. Alternatively, the simpler model simulations may be optimized for different microphysical schemes. This could be achieved by off-line estimation of the weighting factors in the simpler model using the results of

SynPolRad or equivalent model as the reference solution. Both the computational efficiency of SimPolRad and optimization of the simpler reflectivity model will be pursued in near future.

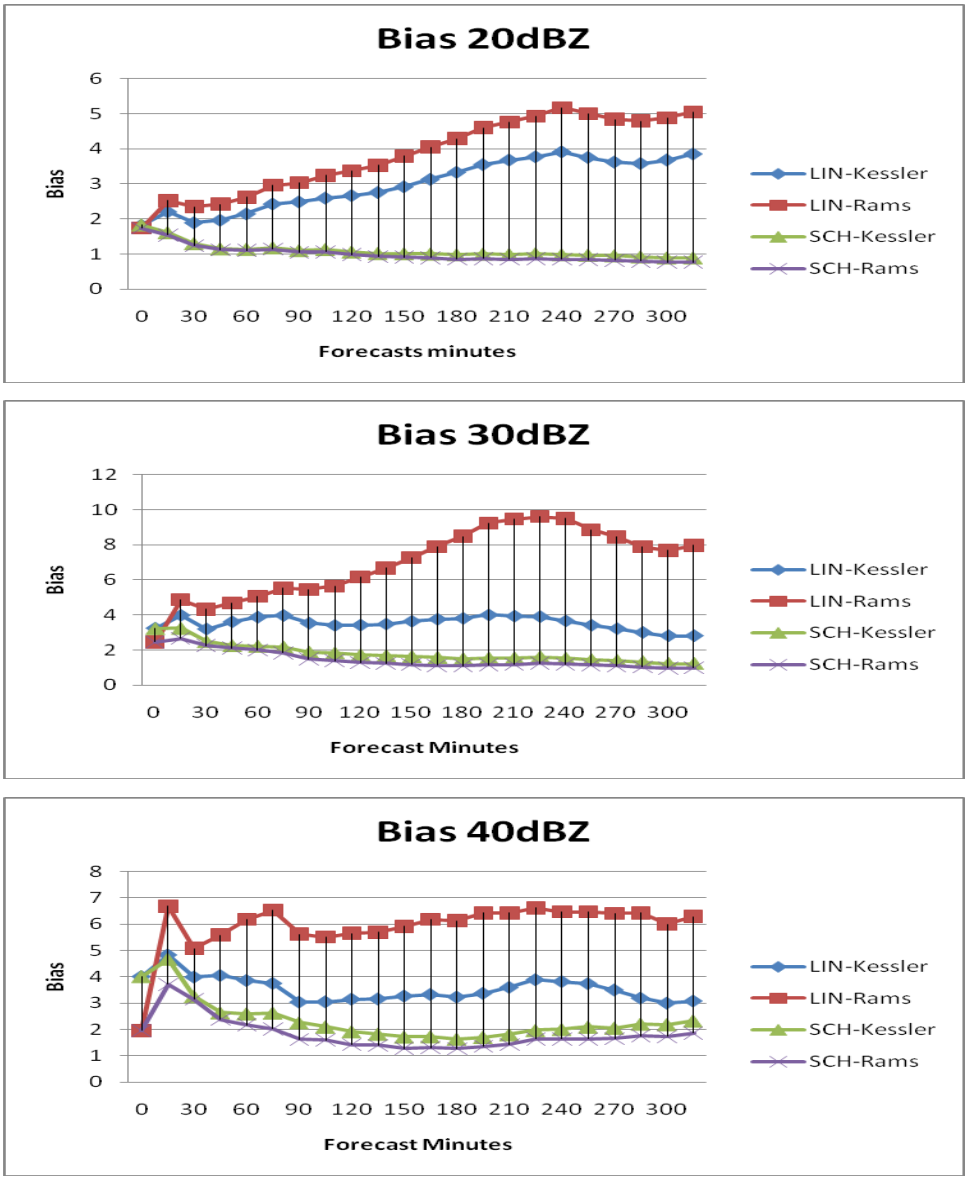


Figure 1. Bias values caluclated for the Lin and Schultz microphysics, for two different refklectivity calculation approaches (Kessler and RAMS) for three reflectivity thersholds and for simulation of June the 13$^{th}$ 2002 event.

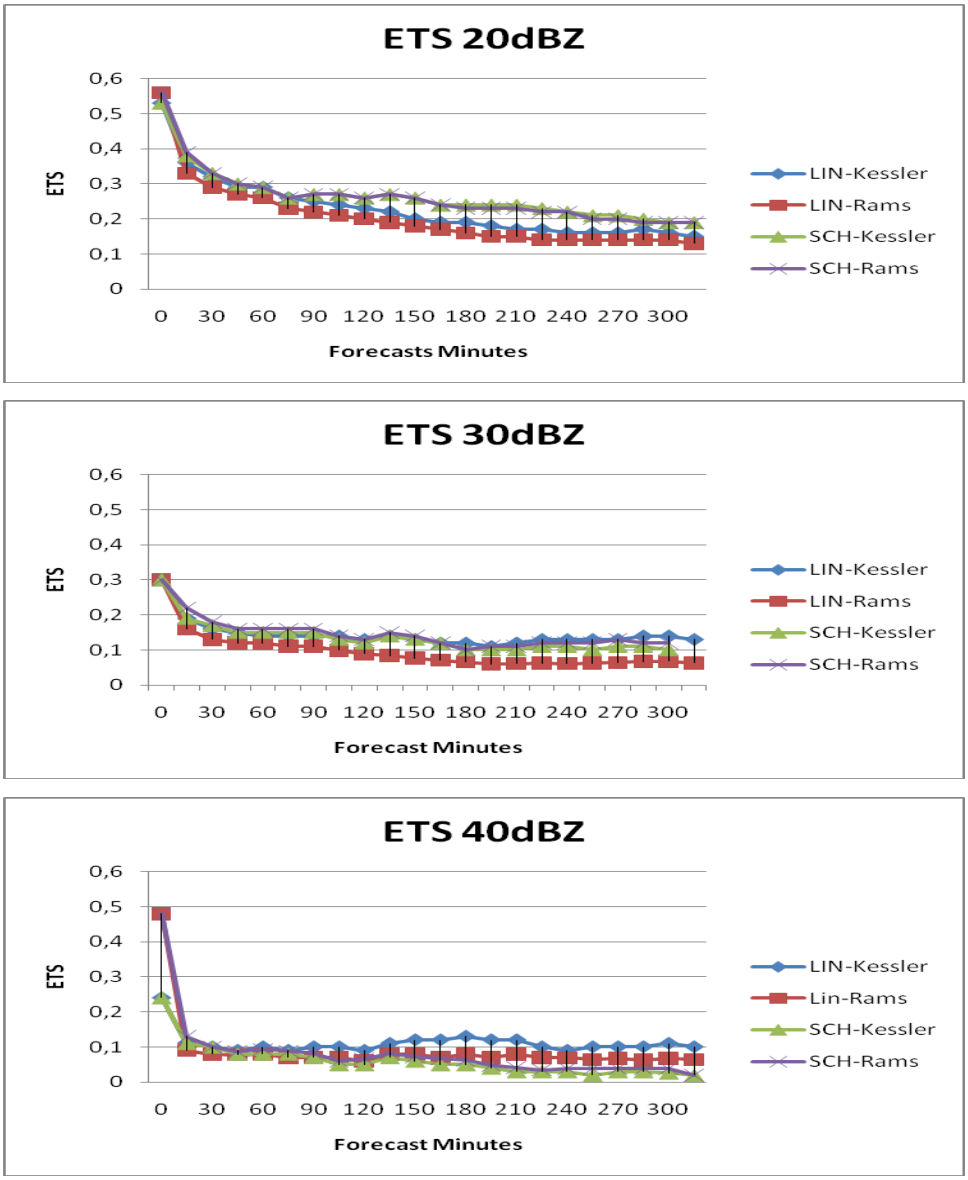


Figure 2. The same as in Fig. 1, except for ETS.

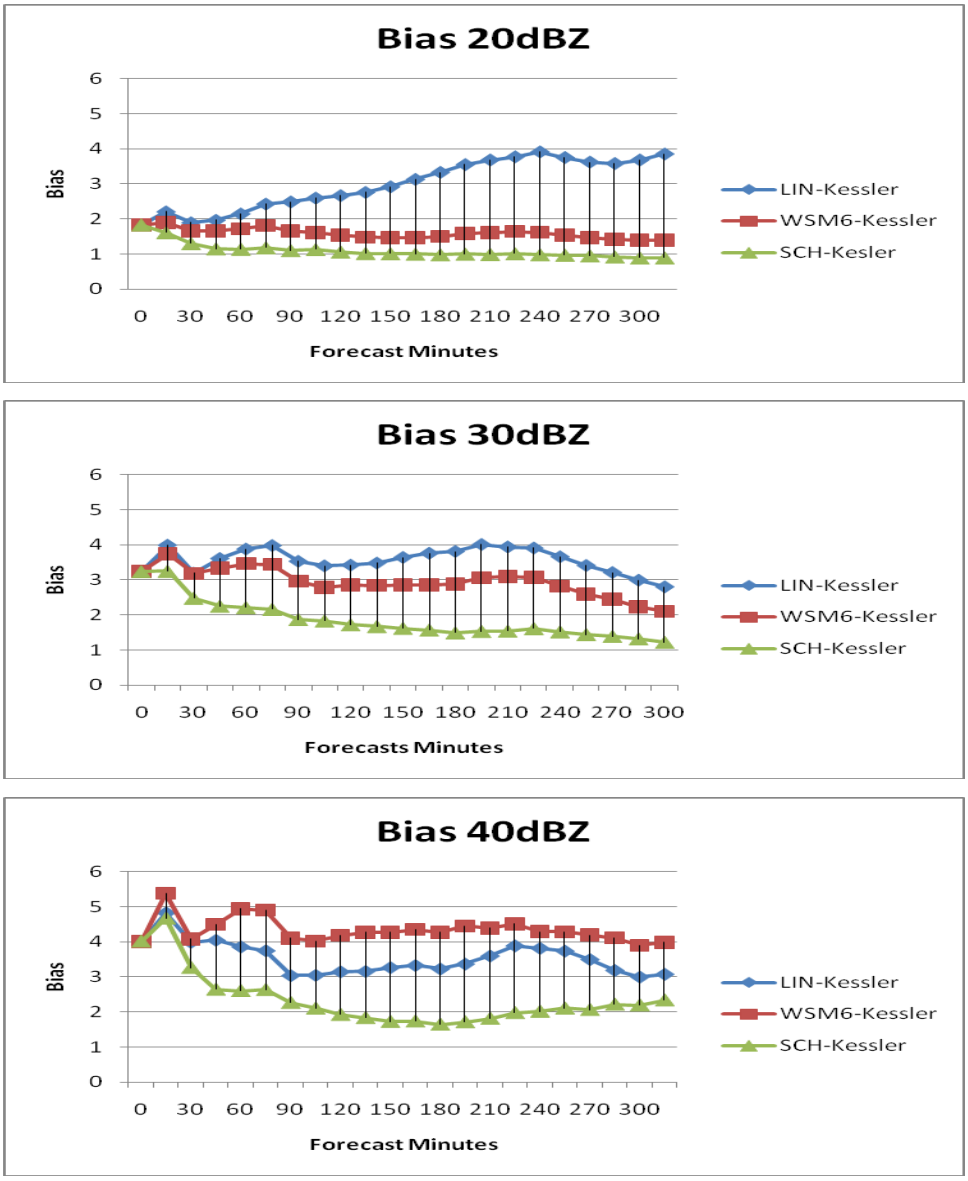


Figure 3. As in Fig.1 except for three different microphysics.

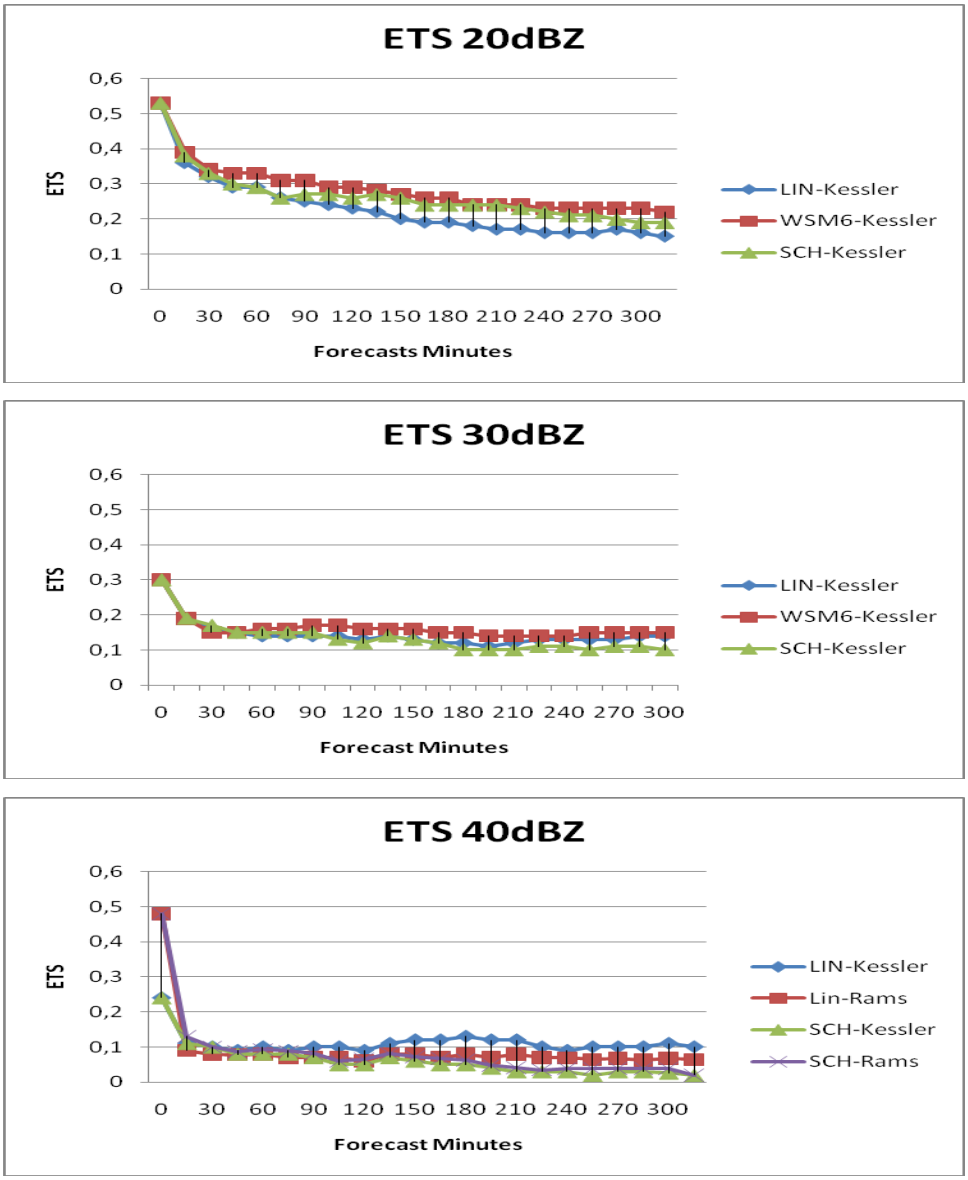


Figure 4. As in Fig. 2 except for three different microphysics.

a) b)

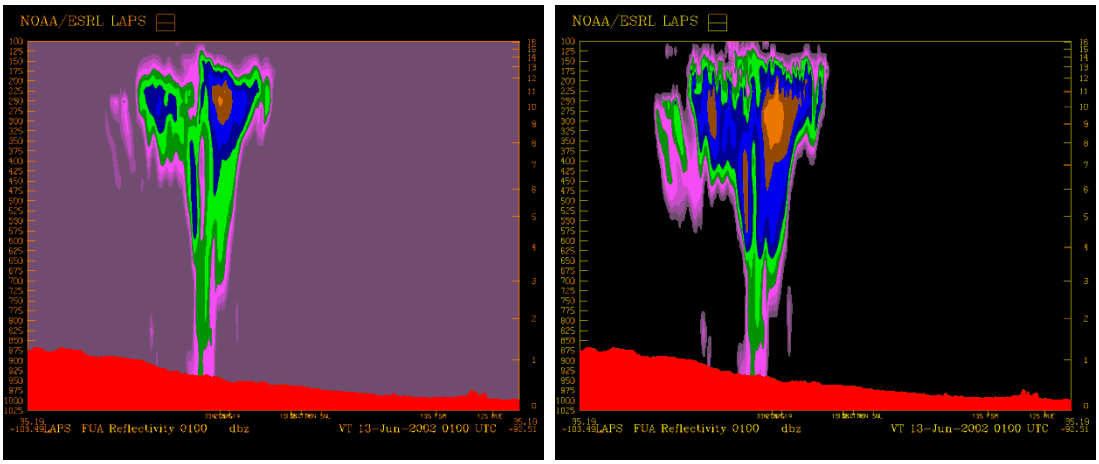


c) d)

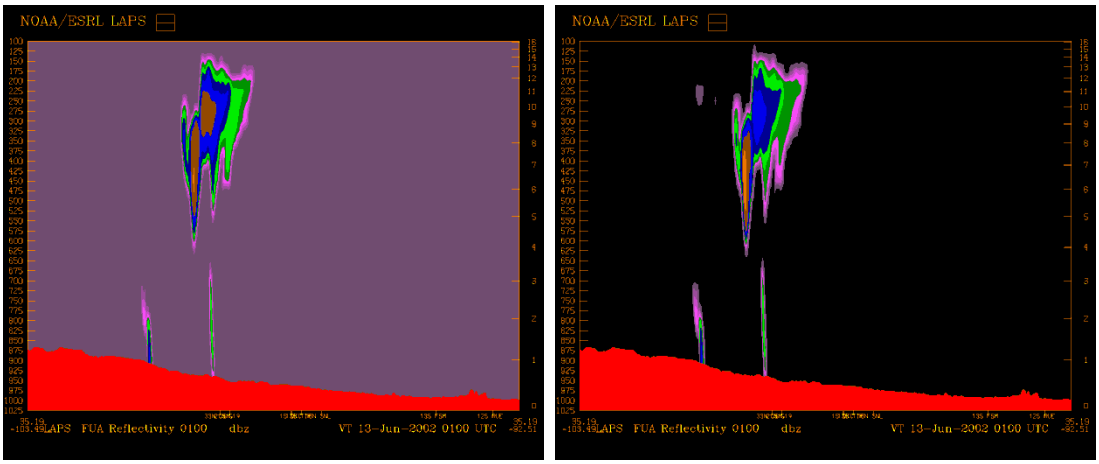


Figure 5. West-East crosssection through the middle of the integration domain of simulated reflectivity by a) Lin microphysics using Kessler, b) Lin microphysics using RAMS, c) Schultz microphysics using Kessler, and d) Schultz microphysics using RAMS reflectivity calculation for the first forecast hour of June the 13$^{th}$ 2002 simulation at 01 UTC.

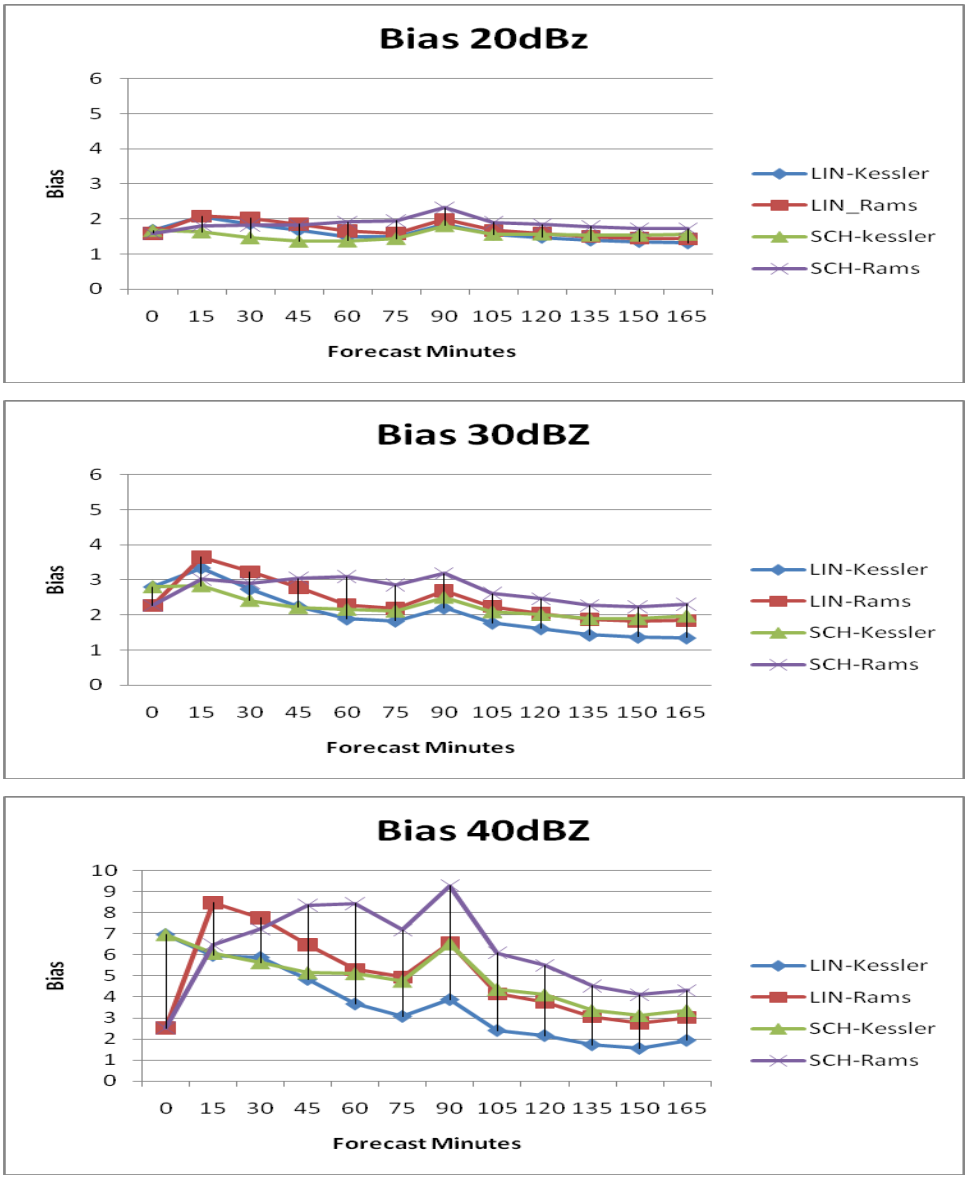


Figure 6. As in Fig.1, except for June the 16th 2002 event.

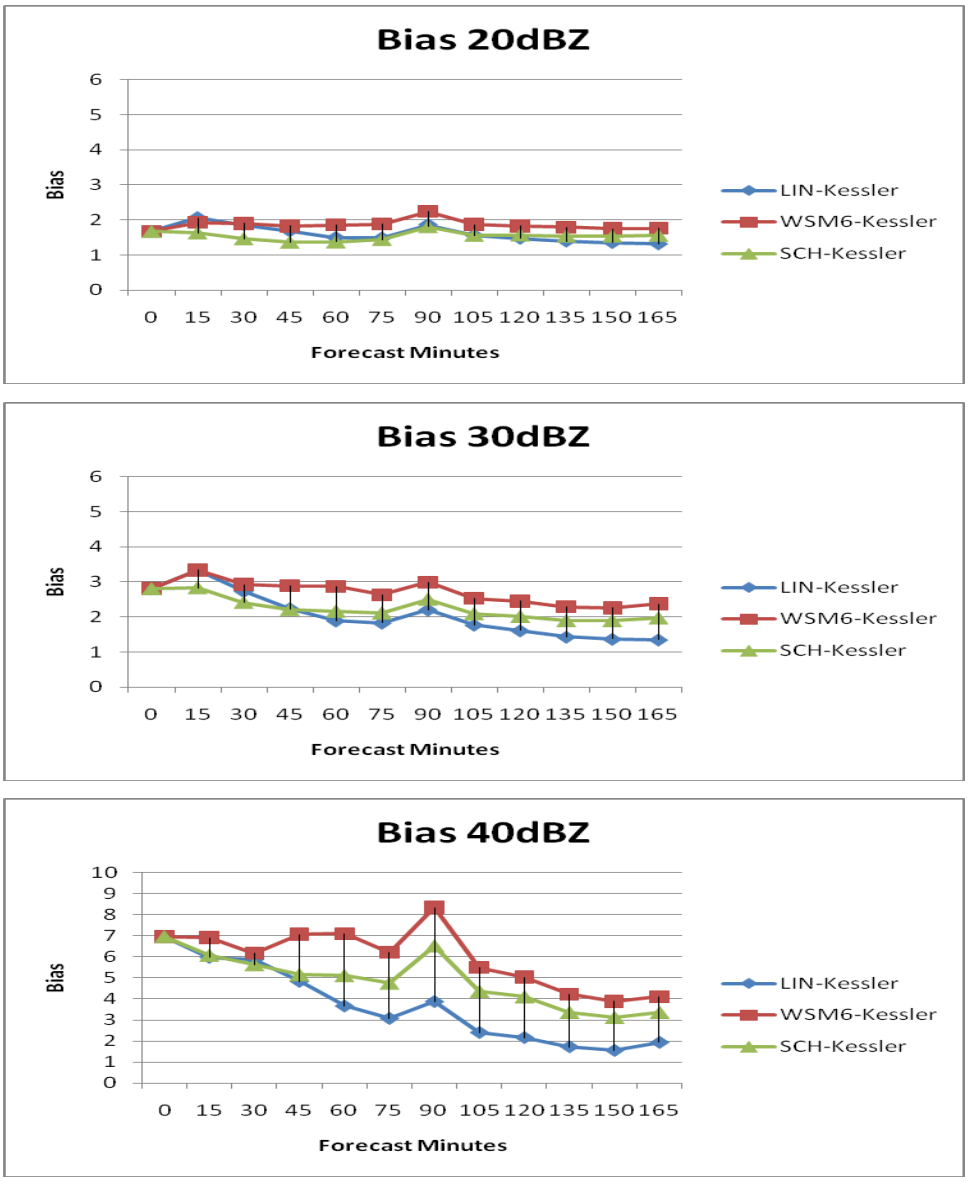


Figure 7. As in Fig. 2, except for June the 16th 2002 event.

a) Lin-RAMS

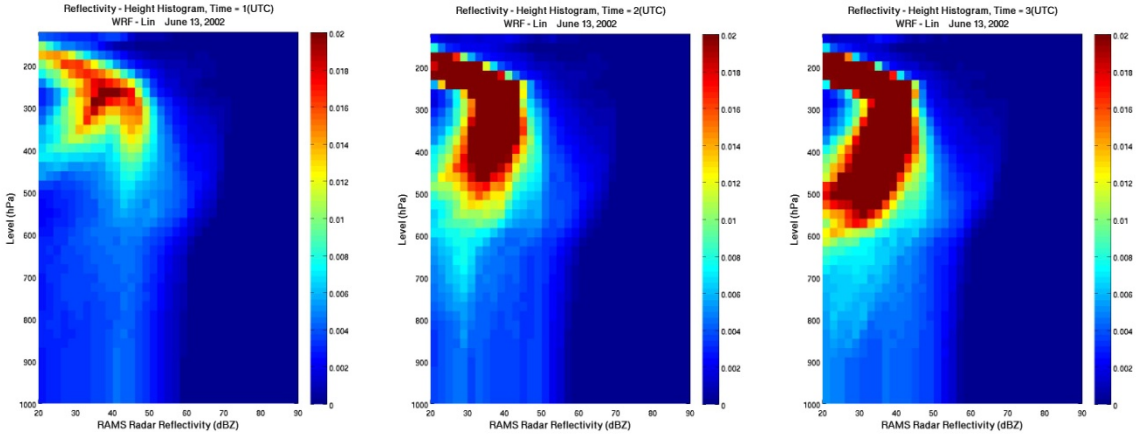


b) Lin-Kessler

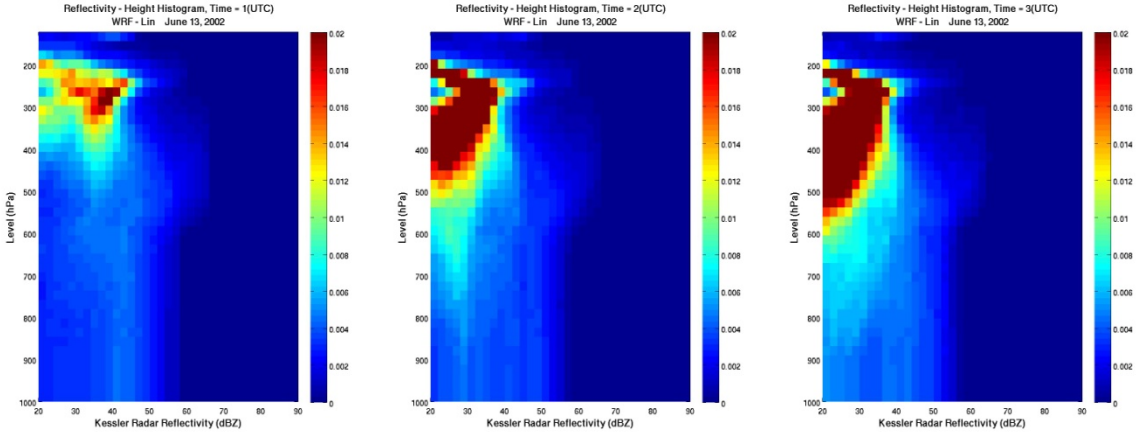


c) Schultz-Kessler

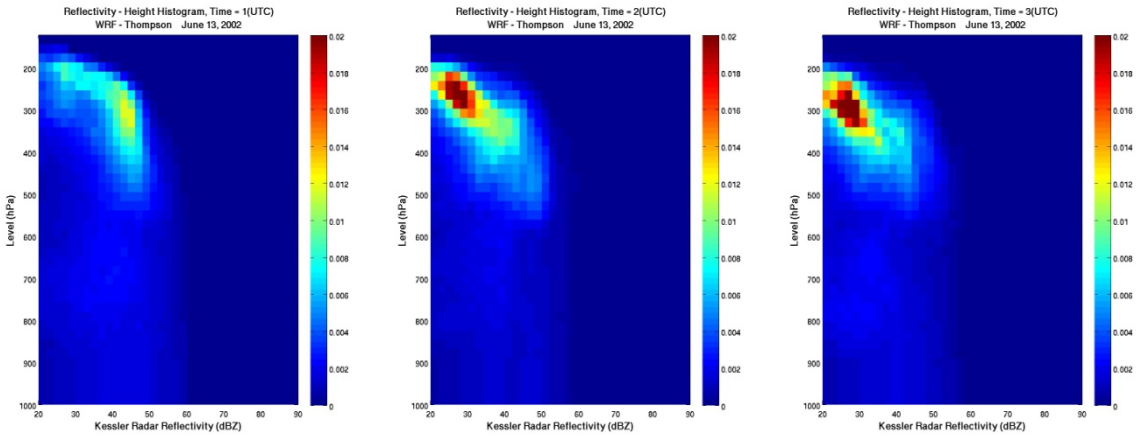


Figure 8. reflectivity-height histograms for a) Lin-RAMS, b) Lin-Kessler, and c) Schultz-Kessler for the first three forecast hours for June the 13$^{th}$ 2002 event.

a) Lin –Kessler

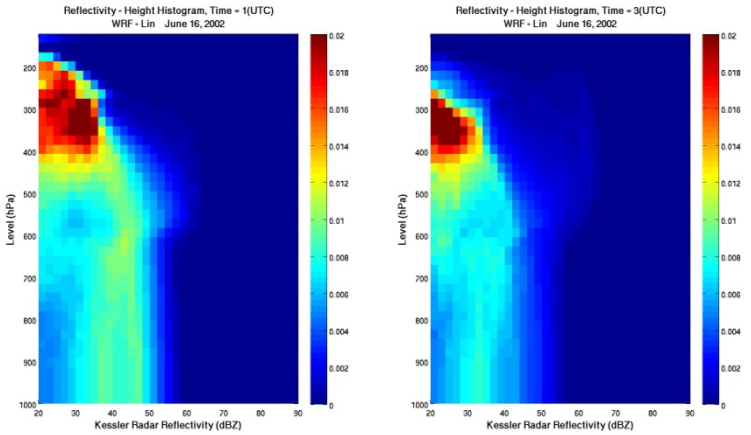


b) Schultz-Kessler

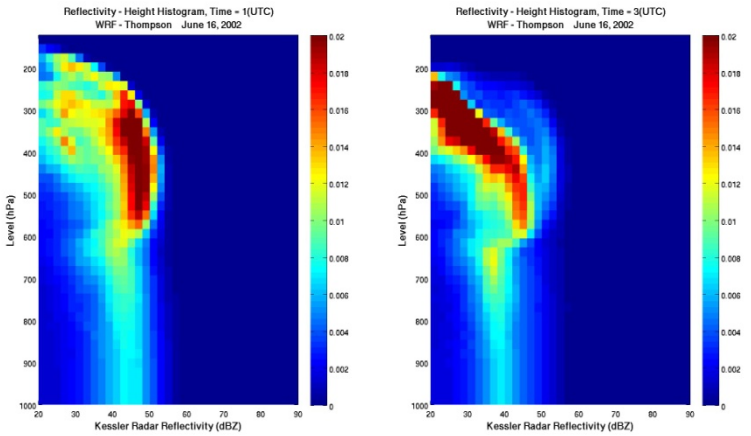


c) WSM6-Kessler

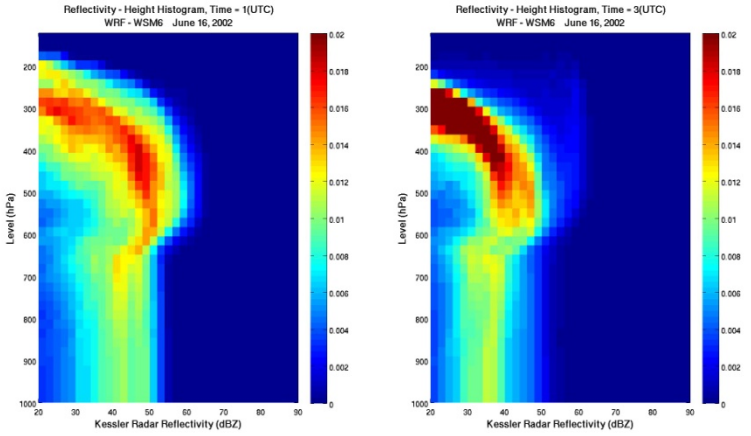


Figure 9. Reflectivity-Height histograms for the three model solutions a) Lin, b)Schultz and c) WSM6 for June the 16$^{th}$ 2002 event and for the 1$^{st}$ and the 3$^{rd}$ forecast hours.

### 3. Evaluating the data assimilation approach using MCMC with 1D cloud resolving model

As explained in the section on major activities we have implemented a 1D lagrangian cloud resolving model with MCMC (Markov Chain Monte Carlo) data assimilation algorithm (Posselt and Vukicevic, 2010) in order to evaluate properties of the radar reflectivity data assimilation problem with respect to the parameterized microphysical processes in terms of favorable conditions that would render the data assimilation problem better constrained and the solutions more accurate when using the data assimilation technique such as 4DVAR (or EnKF, for that matter). A progression of the nonlinear data assimilation problem toward well constrained formulation under varying conditions in the model and observations could be investigated thoroughly only by analysis of the full posterior pdf solutions as shown in Posselt and Vukicevic (2010). Motivated by this approach, the new activity in the project in the second year involved implementation of the 1D model and MCMC algorithm at UM by graduate student van Lier-Walqui and diagnostic analysis of the microphysical processes in the model and simulation of the reflectivity from this model solutions.

The 1D lagrangian cloud model and the MCMC algorithm are described in detail in Posselt and Vukicevic (2010). Only brief summary is presented here. The model is designed to emulate the changes in environment experienced by an atmospheric column as it moves through a cloud system following the mean flow. The vertical profiles of temperature and moisture are fixed and the model is driven by specified time-varying vertical profiles of vertical motion and water vapor tendency. Advection is only allowed to operate on cloud liquid and ice condensate, and only in the vertical direction. By varying the vertical profiles of temperature, moisture, vertical motion, and water vapor forcing, the model can be adapted to simulate the flow through a range of different cloud systems. Since organized deep convection produces the bulk of the warm season precipitation globally, (and over the Great Plains in USA) and has been shown to be highly sensitive to changes in cloud microphysical parameters, an idealized representation of squall line type convection is simulated by the model. The added benefit to examination of squall-line type convection is that it contains two discrete cloud morphologies; convective, in which precipitation is primarily generated by the collision-coalescence (warm rain) process, and stratiform, in which the melting of snow and graupel play a key role. The model is run with 60 vertical layers with constant 250 meter vertical grid spacing and a 5 second timestep, and the radiative transfer,

surface flux, and microphysical parameterizations are all identical to those used in the the NASA Goddard Cumulus Ensemble Model (Tao and Simpson 1993, Tao et al. 2003, Lang et al. 2007). Time series of rain from the model solution over 60 min is shown in Figs. 10 (equivalent to Figure 2a in Posselt and Vukicevic). It can be seen that the model produces realistic time-evolution of a squall-line with the convective phase followed by the stratiform phase.

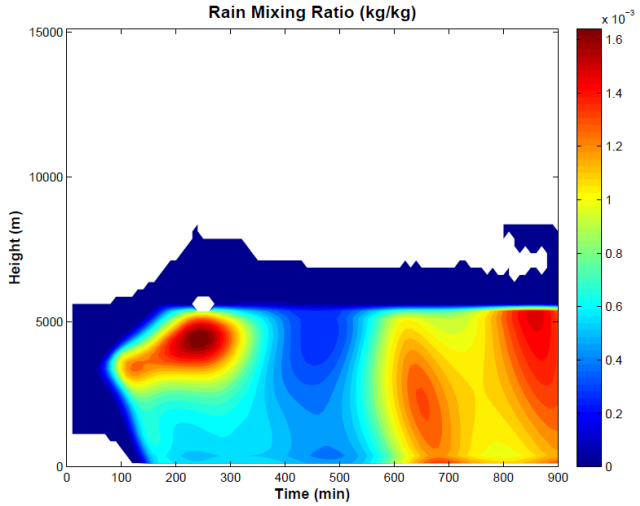


Figure 10. 1D lagrangian model simulation of rain mixing ratio (kg/kg)

The current results using the 1D lagrangian cloud model are preliminary. The results include an initial analysis of the model performance in the microphysical fields and illustration of the diagnostics that would be used in further analysis and data assimilation with the MCMC system. The work leading to the current results was performed over only relatively short period of time during Jan-March 2010, because both the graduate student and PI Vukicevic have been focusing majority of efforts prior to that time to activities related to transitioning to the new appointments.

a) Simulation of reflectivity and polarimetric differential reflectivity using SimPolRad

The radar observation model SimPolRad has been implemented with the 1D modeling system. This observation model enables simulations of radar measurements that are more explicitly sensitive to properties of the hydrometeors including the type, size and shape, than the standard radar measurements. The simulated standard reflectivity and the associated differential reflectivity are

shown in Figure 11. For this simulation the model solution for all liquid and ice hydrometeors are used (not shown).

(a)

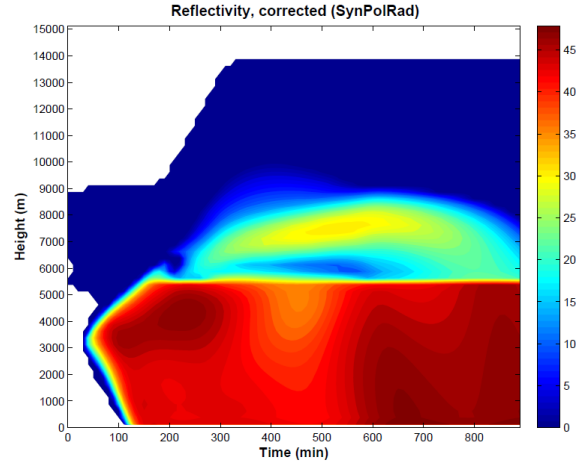


(b)

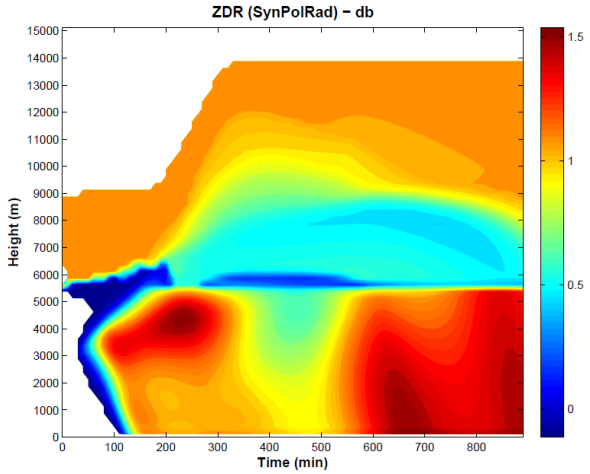


Figure 11: Reflectivity (a) and differential reflectivity (b) from simulated squall line by 1D lagrangian cloud model

The differential reflectivity in Figure 11b shows sensitivity to particles at higher elevation, namely to the snow, which is not evident in the standard reflectivity measurement in Figure 11a. With this capability in the data assimilation system we would study impact of both types of information by the radar measurements with respect to optimizing bulk contribution of the microphysical processes in the model. So far the results simply demonstrate that our modeling system is working properly. We wish to point out that the SymPolRad software must be made more computationally efficient before it is used in MCMC experiments.

b) Analysis of contributions of different microphysical processes

In order to introduce new parameters in the model that would control contribution of different bulk cloud microphysical processes in the data assimilation experiments, the modeled time rate of change by each process and for each prognostic hydrometeor type must be identified in the model software. The identification of the processes in the model code is not trivial as the models are not typically designed for purpose of analysis of the time rate of change by individual processes. Van Lier-Walquie has performed initial "decomposition" of the microphysical scheme in the 1D-lagrangian model. The preliminary results are illustrated in Figure 12. This figure shows contributions of different processes to the time rate of change of the modeled rain. The rates are vertically integrated at each model time step. The results in Figure 12 show that dominant process for the rain production in the model is the accretion of cloud water by rain (red curve). This result is expected, especially during the convective phase (up to 400 time steps on the time axis). However, the peak values during the stratiform phase (after 500-th time step) seem relatively too high because they are compatible with the values during the convective phase. On the other hand, steady increase of melting of snow to rain is depicted realistically in the model during the stratiform phase, at least in terms of trend. The reality of actual magnitude of the melting time rate of change cannot be evaluated because it is not known.

We have performed the equivalent analysis of contributions of different processes for each other prognostic hydrometeor type in the model (not shown). We are currently evaluating accuracy of the data in these analyses in terms of making sure that the correct data are being extracted from the model simulation. As mentioned above, the model algorithm is not designed to evaluate time tendency terms that are produced by the individual microphysical processes. Consequently, special data output must be devised and tested for the purpose of our analysis. Once the adequacy of data is confirmed, the results that are illustrated in Figure 12 and equivalent for the other hydrometeors would be used to define a set of control parameters in the data assimilation by MCMC with the radar reflectivity observations. In addition, the evolution of time rate of change by individual processes would be used as one of standard diagnostics when

evaluating impact of data assimilation to the modeling of the bulk microphysics.